ELSEVIER

Journal of Nuclear Materials 270 (1999) 233–241

journal of nuclear materials

On the zirconium–oxygen–hydrogen ternary system

Masanobu Miyake [a], Masayoshi Uno [b], Shinsuke Yamanaka [b,*]

[a] *Fukui University of Technology, Gakuen 3-6-1, Fukui 910, Japan*

[b] *Department of Nuclear Engineering, Faculty of Engineering, Graduate School of Engineering, Osaka University, Yamadaoka 2-1, Suita, Osaka 565, Japan*

Received 18 June 1998; accepted 22 September 1998

Abstract

Thermodynamic studies on the Zr–O–H ternary system have been carried out, based on the hydrogen solubility for αZr(O), βZr(O) and ZrO_2. The dissolved oxygen in zirconium strongly affected both the hydrogen solubility and the phase diagram. The effect of the interstitial oxygen on the hydrogen solubility was discussed on the basis of the partial molar quantities of hydrogen in the Zr–O–H ternary solid solutions. The hydrogen dissolution into the ZrO_2 was studied in O_2/H_2O atmosphere using a thermal desorption method. The hydrogen solubility in the ZrO_2 was evaluated from the thermal desorption spectra to range from 10^{-5} to 10^{-4} mol H/mol oxide and decreased with increasing temperature.

1. Introduction

Zirconium alloys such as Zircaloy and Zr–Nb have been used as the cladding materials of light water reactors (LWRs). In recent years, the renewed interest in hydrogen behavior in the cladding under normal and accident conditions of LWRs promotes reassessment of the zirconium–hydrogen system.

The chemical thermodynamics for the Zr–H binary system have been extensively studied [1–8] and reviewed [9–11]. However, limited data are available for the hydrogen solubility in zirconium at high temperatures and there exists a little information on gaseous contaminants such as oxygen on the hydrogen solubility in zirconium [12]. Insufficient information is available for hydrogen dissolution into zirconium oxide [13].

Therefore, the authors have reexamined the hydrogen solubility and the phase relationship in the Zr–H system and studied the influence of interstitial oxygen on hydrogen solubility in zirconium [14–18]. Thermochemical studies on the hydrogen dissolution into ZrO_2 oxide have been also carried out [19]. The present paper describes the results for the Zr–O–H ternary system obtained in recent years.

2. Experimental

The hydrogen solubility in zirconium–oxygen solid solutions was studied using a modified Sieverts' UHV apparatus. The solubility was evaluated from change in pressure with dissolution of hydrogen gas into the solid solution at constant volume. The measurement was performed at a temperature of 600–1050°C at a pressure below 10^4 Pa by a constant volume method. Details of experimental conditions and specimens were described in our previous paper [14,18].

The sintered ZrO_2 oxide with a monoclinic structure was exposed to a flow of wet oxygen in the temperature range of 500–1000°C. The water vapor pressure was controlled to be 872 Pa, and the total pressure of the gas mixture of oxygen and water vapor was 10^5 Pa. A total amount of hydrogen absorbed in the specimen was measured by means of a thermal desorption method. The experimental apparatus and procedure will be published elsewhere [19].

3. Hydrogen solubility in Zr(O) solid solutions

All the solubility data for the hcp αZr(O) and bcc βZr(O) solid solutions closely obey Sieverts' law:

$$C_H = K_H \times P_{H_2}^{1/2}, \quad (1)$$

* Corresponding author. Tel.: +81-6 879 7887; fax: +81-6 875 5696; e-mail: yamanaka@nucl.eng.osaka-u.ac.jp.

0022-3115/99/$ – see front matter
PII: S0022-3115(98)00779-X

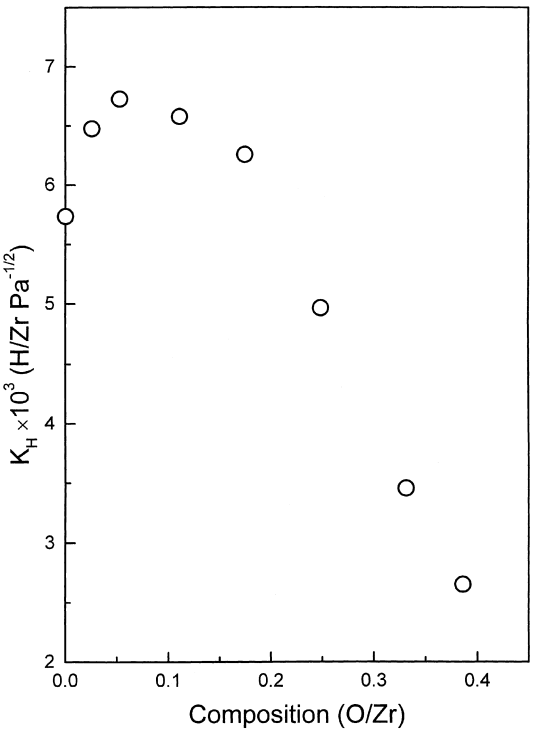

Fig. 1. Change in the Sieverts' constant K_H for the αZr(O) solid solution with the oxygen content [14].

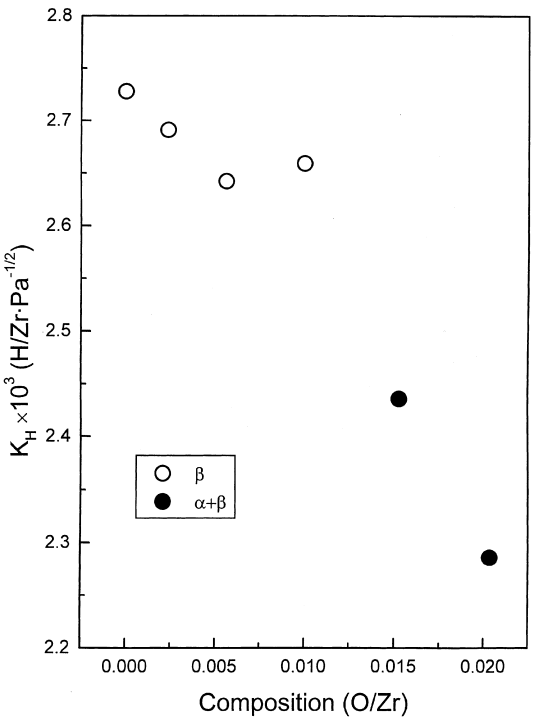

Fig. 2. Change in the Sieverts' constant K_H for the βZr(O) solid solution with the oxygen content [18].

where C_H is the hydrogen content in atom ratio (H/Zr), P_{H_2} the equilibrium hydrogen pressure in Pa, and K_H the Sieverts' constant. As shown in Fig. 1 [14], the hydrogen solubility in the αZr(O) solid solution at 700°C goes through a maximum at an O/Zr ratio of 0.1, and decreases with increasing oxygen content above 0.1 O/Zr. The hydrogen solubility in the βZr(O) solid solution at 1000°C first decreases with the oxygen content and then increases slightly, as evidenced by Fig. 2 [18]. This trend for βZr(O) differs from that for αZr(O).

The temperature dependence of the Sieverts' constant for the αZr(O) is illustrated in Fig. 3 [14], showing the following relationship holds between the Sieverts' constant K_H and the reciprocal temperature $1/T$ (K):

$$\ln K_H = A + B/T, \tag{2}$$

where A and B are constants. The enthalpy of solution of hydrogen ΔH (kJ/mol) can be evaluated from the B value. It is obvious from this figure that the αZr(O) solid solutions with the oxygen contents below 0.0176 O/Zr have larger hydrogen solubility than pure zirconium and that the presence of interstitial oxygen varies the enthalpy of solution. The temperature dependence of Sieverts' constant obtained for the βZr(O) solid solutions is shown in Fig. 4 [18]. Linear relationships between ln K_H and $1/T$ are found to hold for βZr(O) solid solutions

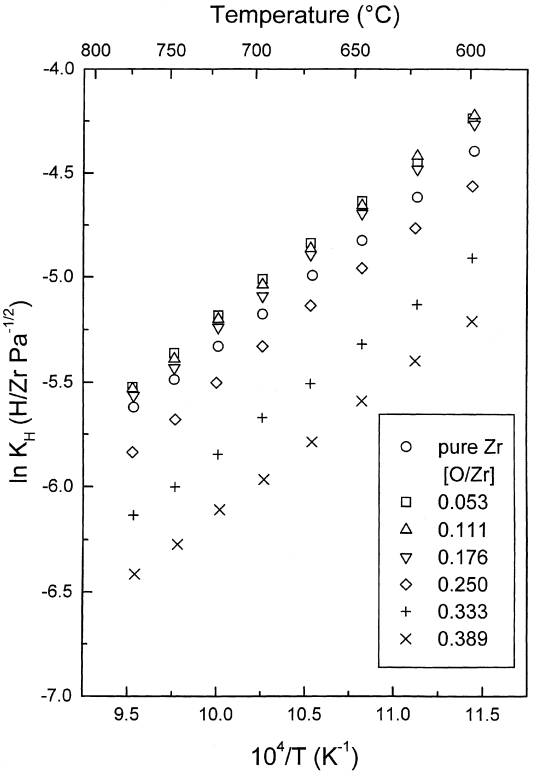

Fig. 3. Temperature dependence of Sieverts' constant K_H for the αZr(O) solid solution [14].

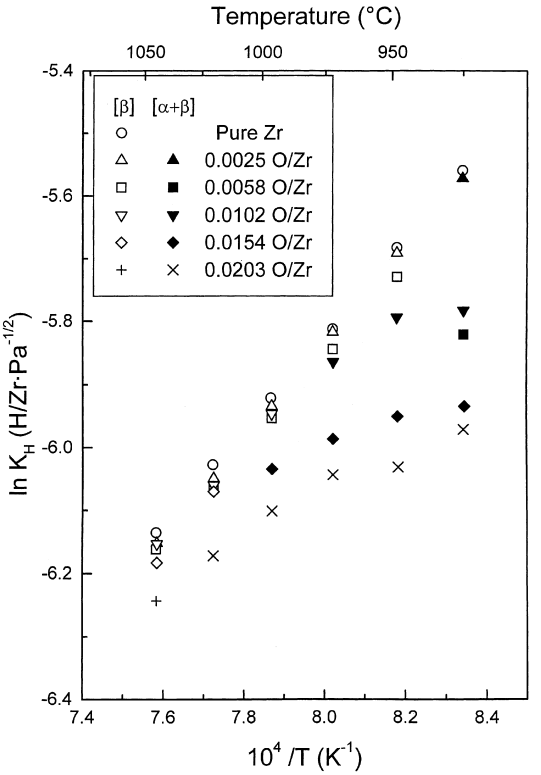

Fig. 4. Temperature dependence of Sieverts' constant K_H for the βZr(O) solid solution [18].

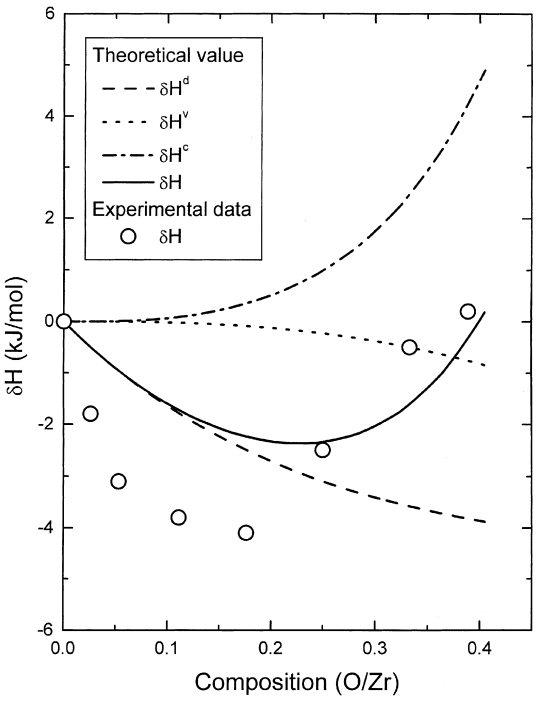

Fig. 5. Thermodynamic analysis of the change in the δH value with the oxygen content of αZr(O).

with the oxygen contents below 0.01 O/Zr. There is no linear relationship for alloys with higher oxygen contents. This suggests that the Zr(O) below 0.01 O/Zr is the single β phase and the Zr(O) with higher oxygen contents are in the two-phase region of α + β. For βZr(O), the enthalpy of solution first decreases and then increases as the oxygen content increases.

4. Thermodynamic analysis for Zr–O–H ternary solid solutions

The authors assumed that hydrogen atoms have access to tetrahedral interstitial sites in a zirconium metal lattice and applied the following solubility equation to the solubility data for the Zr(O) solid solutions,

$$\ln\left(C_H T^{7/4}/(\beta - C_H)P_{H_2}^{1/2}A_{H_2}\right) = -(H_H - E^d)/kT + S_H/k, \quad (3)$$

where H_H and S_H are the partial molar enthalpy and the partial molar excess entropy of hydrogen referred to the standard state of hydrogen atoms at rest in a vacuum, E^d the one half of the dissociation energy of the hydrogen molecule, k the Boltzmann constant, and A_{H_2} the value related to partition functions of hydrogen gas. The value of β is the number of interstitial sites of given kind available to hydrogen per zirconium atom. For the hcp α phase, $\beta = 2$ and for the bcc β phase, $\beta = 6$.

In order to clarify the influence of interstitial oxygen, the solubility data for αZr(O) and βZr(O) solid solutions were analyzed by applying Eq. (3) to the solubility data. The changes in the solubility and the enthalpy of solution with addition of interstitial oxygen were discussed in terms of the difference in partial molar enthalpy and excess entropy between pure zirconium and solid solution, which are defined as $\delta H = H_H - H_H^0$ and $\delta S = S_H - S_H^0$ where H_H and S_H are the values for the oxygen solid solutions and H_H^0 and S_H^0 for pure zirconium. Figs. 5–8 show the changes in δH and δS values with the oxygen content of the solid solution. As shown in these figures, the δH and δS first decrease with the oxygen content and then markedly increase at higher oxygen contents. The change in the solubility in Zr(O) alloys is attributable to a net result from the variation in δH and δS. The effects of interstitial oxygen on partial molar quantities are significantly different from bcc βZr(O) to hcp αZr(O).

The changes in δH and δS with the oxygen content in αZr(O) and βZr(O) on the assumption that the enthalpy and entropy difference δH and δS were given by the sum of various contributions: $\delta H = \delta H^v + \delta H^d + \delta H^c$ and

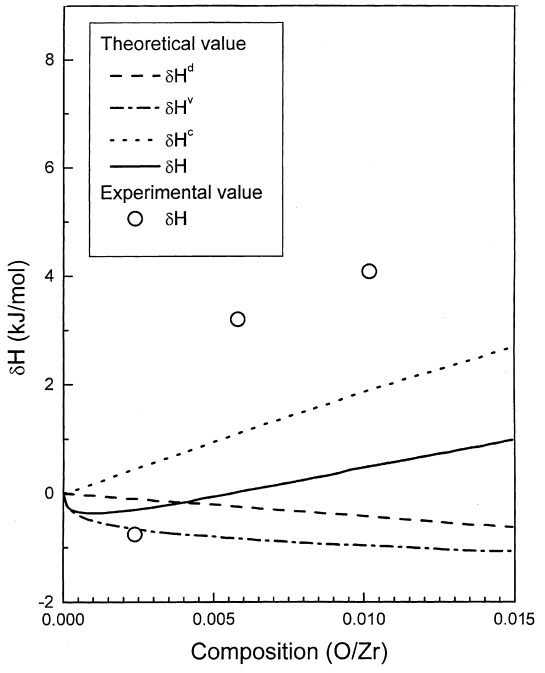

Fig. 6. Thermodynamic analysis of the change in the δH value with the oxygen content of βZr(O).

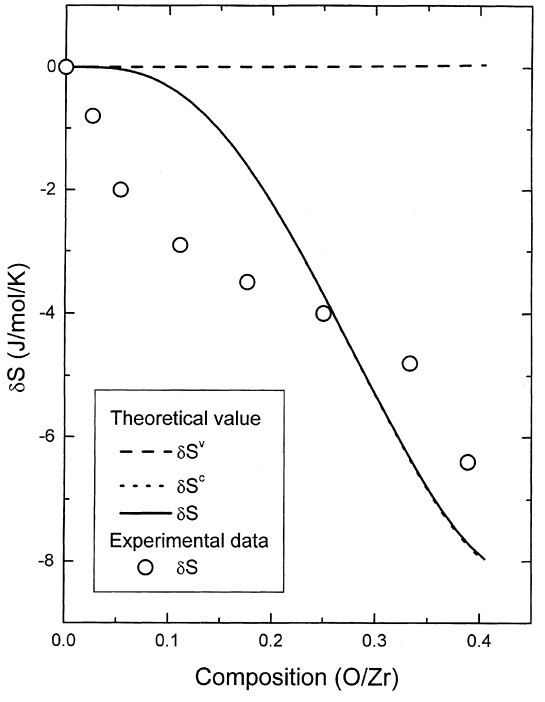

Fig. 7. Thermodynamic analysis of the change in the δS value with the oxygen content of αZr(O).

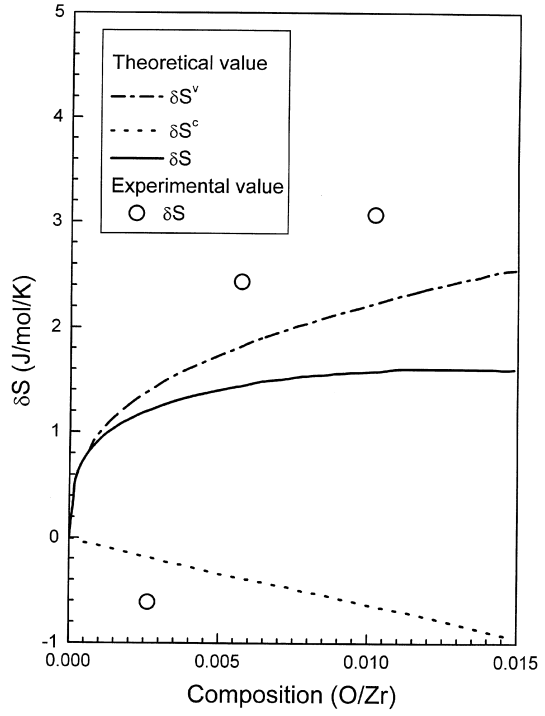

Fig. 8. Thermodynamic analysis of the change in the δS value with the oxygen content of βZr(O).

$\delta S = \delta S^{v} + \delta S^{d} + \delta S^{c}$ where δH^{v} and δS^{v} are the differences in vibrational contribution between the alloy and pure zirconium, δH^{d} and δS^{d} the lattice dilatation terms, and δH^{c} and δS^{c} the configurational terms. The results for the analysis are shown in Figs. 5–8. The method for the analysis was reported in detail elsewhere [16].

As shown in these figures, the δH^{v} is small and negative, and δS^{v} is small and positive. The values of δH^{v} and δS^{v} obtained for αZr(O) are larger than those for αZr(O). As evidenced by these figures, the volume expansion due to interstitial oxygen results in a negative enthalpy change, and the value of δS^{d} is negligibly small. There is no marked difference in the volume effect between αZr(O) and βZr(O), as shown in Figs. 5–8. Figs. 7 and 8 show that δS^{c} shows a negative value and decreases with the oxygen content for both αZr(O) and βZr(O). The trend in δH^{c} and δS^{c} for βZr(O) is almost the same as αZr(O). The theoretical curves shown by solid lines in Figs. 5–8 demonstrate the tendency for the changes in the experimental δH and δS values with oxygen addition into zirconium.

In Fig. 9, the configurational term δH^{c} thus estimated is compared with other physico-chemical properties of the αZr(O) solid solution. As obvious in Fig. 9(b), oxygen is an α stabilizing element for zirconium, and the Zr(O) solid solutions with a hcp α phase have congruent melting points, temperature of which is

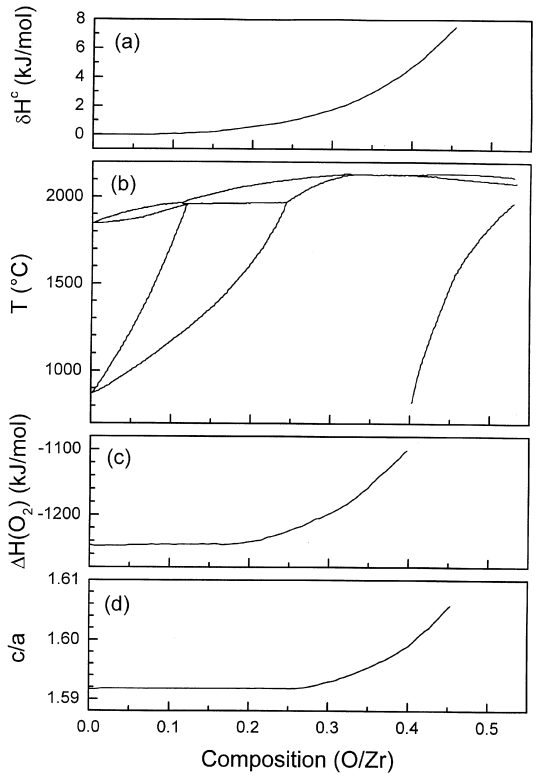

Fig. 9. Comparison of the δH value with other properties of the αZr(O) solid solution.

much higher than melting point of pure zirconium. This suggests that oxygen increase the thermodynamic stability of the solid phase and that strong chemical interaction occurs between oxygen and zirconium in the solid solutions. The strong interaction of oxygen with zirconium appears to cause a change in the hydrogen–zirconium interaction, and hence it may vary the configurational enthalpy of hydrogen in solid solutions. It should be noted that there exists a good correlation between δH^c values and the physical properties of the Zr(O) solid solution. The trends of the change in δH^c with oxygen content well agree with the composition dependence of the partial molar enthalpy of oxygen for binary oxygen solid solution. Axial ratios of c/a are considered to reflect electronic properties of an hcp metal. The changes in the c/a ratio for Zr(O) solid solutions are also in agreement with δH^c -composition relationships. The marked increase of δH^c at a higher oxygen content appears to be closely related to the change in characteristics of Zr(O) solid solutions. We may have a knowledge about microproperties of metals in a binary solution from configurational terms which can be estimated from hydrogen solubility measurement.

5. Phase diagram of Zr–O–H ternary system

Fig. 10 indicates the isothermal section of the Zr–O–H ternary system at 700°C constructed from the equilibrium hydrogen pressure–hydrogen concentration isotherms for the Zr(O) solid solutions. In the isothermal section at 700°C, there exists a characteristic triangle representing the α + β + δ three-phase region. Compositions of the solid phases and hydrogen pressure are thermodynamically fixed in this three-phase region. This three-phase region is adjacent to two-phase regions of α + β, β + δ, and α + δ. The tie lines in the isothermal section connect the conjugate phases in the two-phase regions. The terminal solubility of hydrogen in the α phase is slightly increased by the presence of oxygen, and oxygen has a lower solubility in the β and δ phases than in the α phase. These features are consistent with literature data at a higher temperature [1]. Though Ells and McQuillan [1] have proposed that at 750°C solute oxygen in zirconium stabilizes the α phase up to a hydrogen content of 0.3 H/(Zr + O + H), our data show a smaller stabilizing effect of oxygen for α phase.

6. High temperature hydrogen solubility in Zr

In LWRs, the corrosion of the cladding results in the formation of ZrO_2 oxide on the surface of the cladding, and a metallic phase inside the oxide appears to be αZr(O) solid solution according to the Zr–O binary phase diagram [20]. Since the cladding temperature is below 400°C under the normal operating conditions of LWRs, the hydrogen solubility in the Zr(O) at temperatures below 400°C is required to estimate the penetration of hydrogen into the cladding and the hydrogen distribution in the cladding. Under the accidental conditions of LWRs, the cladding temperature may increase above 1000°C. The hydrogen solubility at higher temperature above 1000°C is of importance to evaluate the generation rate of hydrogen due to reaction of water vapor with the cladding. Hydrogen behavior may be associated with the fuel–cladding interaction and the fission product release from the fuel rod. Therefore, the hydrogen solubility in the α and βZr(O) solid solution was estimated from the experimental results.

The experimental conditions of the solubility measurement such as the oxygen content in the Zr(O) and the temperature range are indicated in the phase diagram of the Zr–O binary system, as shown in Fig. 11. The estimated values of hydrogen solubility in Zr(O) are shown in Figs. 12 and 13. The hydrogen solubility at 400°C corresponding to the operating temperature of the cladding is one order of magnitude larger than that at 600°C. The effect of oxygen is much higher for 400°C than for higher temperatures. The solubility for the αZr(O) with about 0.1 O/Zr is twice as much as that for pure

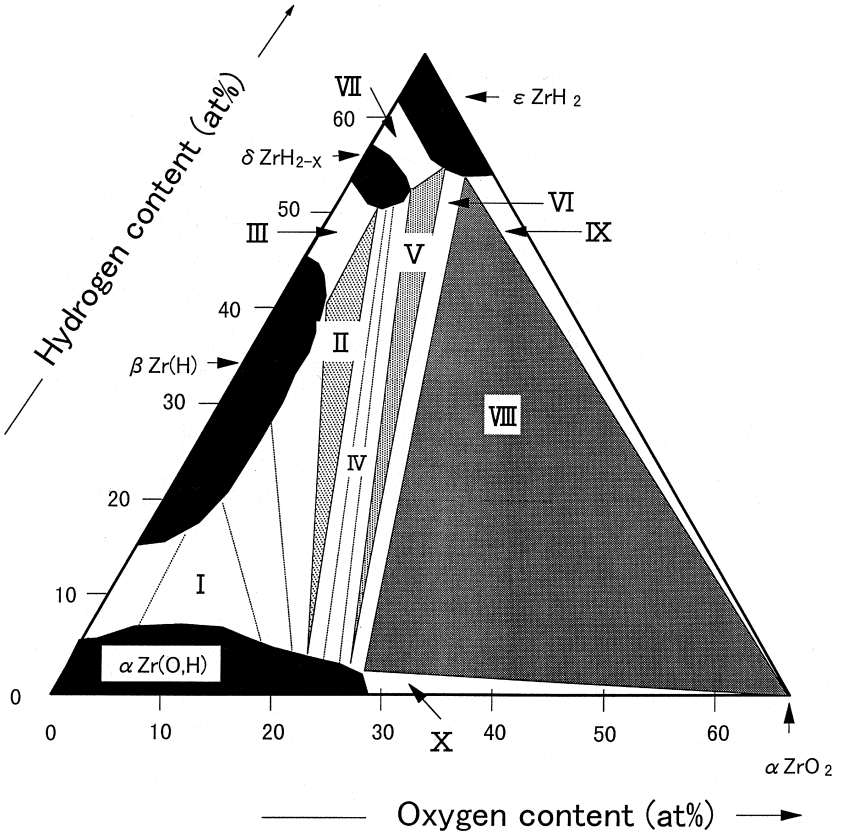

Fig. 10. Isothermal section of the Zr–O–H ternary system at 700°C. I. α + β, II. α + β + δ, III. β + δ, IV. α + δ, V. α + δ + ε, VI. α + ε, VII. δ + ε, VIII. α + ε + ZrO_2, IX. ε + α ZrO_2, X. α + α ZrO_2.

zirconium and markedly decreases with increasing oxygen content. Post-irradiation examination of Zircaloy cladding indicated that complicated hydrogen distribution was observed in the cladding. Hydrogen transport in the cladding is determined by a gradient in chemical potential of hydrogen. Monotonical decrease in the hydrogen concentration from the surface of the cladding to the inside was not anticipated from the results estimated in the present study. Above 1000°C, the effect of oxygen on hydrogen solubility in αZr(O) becomes smaller. For the βZr(O), the change in the hydrogen solubility with the oxygen content is smaller than for αZr(O). The change in the temperature from 1000°C to 1800°C decreases the hydrogen solubility one order of magnitude lower. At temperatures above 1000°C, the hydrogen solubility is not zero, and even at 1800°C zirconium can absorb hydrogen up to 0.3 H/Zr at 1 MPa.

7. Hydrogen dissolution in ZrO_2 oxide

The hydrogen dissolution into the monoclinic ZrO_2 was studied in the temperature range of 500–1000°C in oxygen/water vapor atmosphere [19]. The hydrogen containing species released from the ZrO_2 was H_2O and negligibly small amount of H_2 was released from the ZrO_2. The total amount of dissolved hydrogen in the ZrO_2 was evaluated from the thermal desorption spectra, which enabled us to estimate the hydrogen solubility in ZrO_2. The hydrogen solubilities in the ZrO_2 were found to be from 10^{-5} to 10^{-4} mol H/mol oxide.

The dependence of the hydrogen solubility on the temperature is illustrated in Fig. 14, together with the literature data [21–26]. It is found from this figure that the hydrogen solubility in the ZrO_2 oxide obtained in the present study slightly decreases with increasing temperature. The hydrogen solubility in the monoclinic ZrO_2 oxide obtained in the present study is close to the solubility data for other oxides such as cubic and tetragonal ZrO_2 [13,22]. The equilibria between the atmosphere and the zirconium oxide were able to be explained in terms of reaction involving oxygen vacancy and interstitial hydrogen defect [19]. Estimates of equilibrium constants for the hydrogen defect formation were described in detail elsewhere [19].

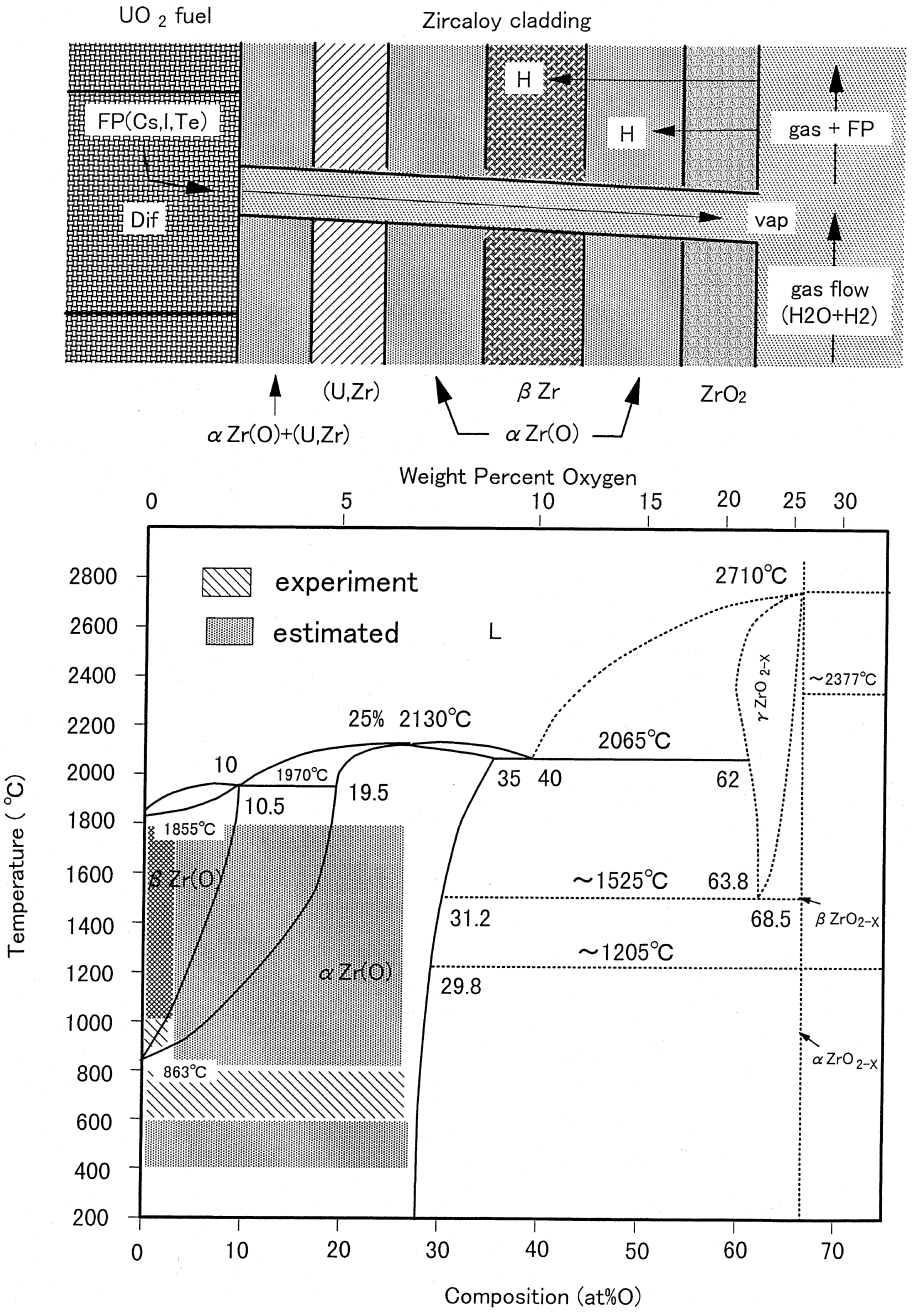

Fig. 11. Experimental conditions indicated in the phase diagram of the Zr–O binary system.

8. Summary

Thermodynamic studies have been performed on the Zr–O–H ternary system through measurements of hydrogen solubility for hcp αZr(O) and bcc βZr(O) solid solutions and for ZrO_2 oxide.

The hydrogen solubility for hcp α phase first increased with the oxygen content and then decreased at higher oxygen contents. The hydrogen solubility in the βZr(O) solid solution first decreased with the oxygen content and then increased slightly. The presence of interstitial oxygen varied the enthalpy of solution of hydrogen into both the αZr(O) and βZr(O) solid solutions. The influence of the interstitial oxygen was discussed on the basis of the partial molar quantities of hydrogen in Zr(O) solid solutions derived from the experimental data.

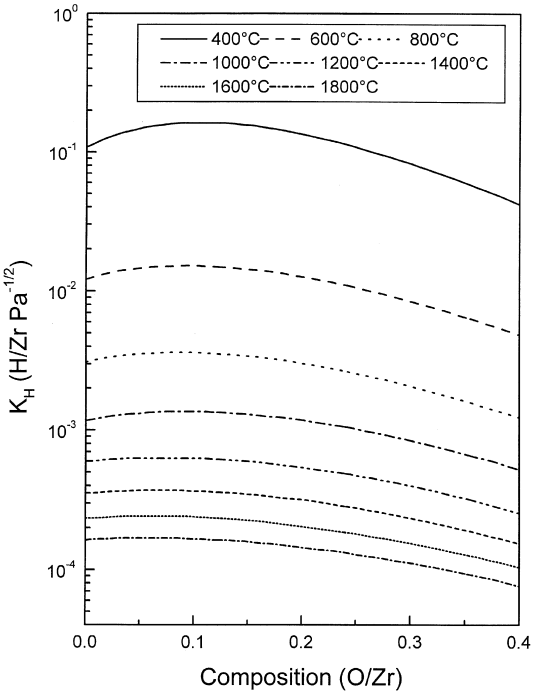

Fig. 12. Estimated Sieverts' constant K_H for the αZr(O) solid solution.

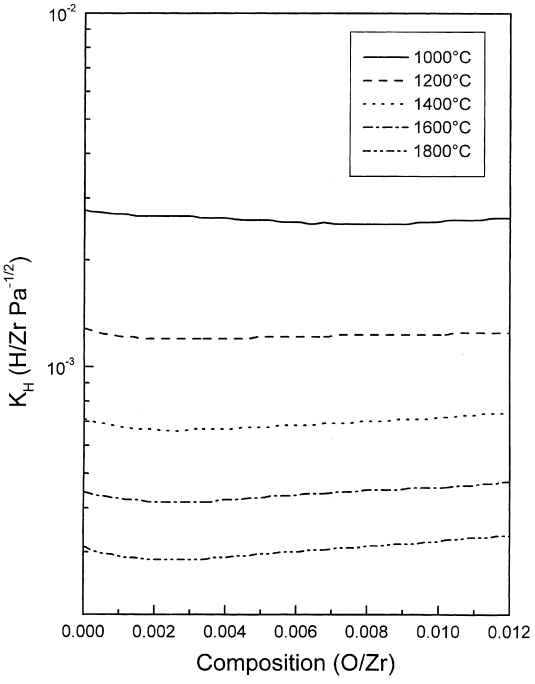

Fig. 13. Estimated Sieverts' constant K_H for the βZr(O) solid solution.

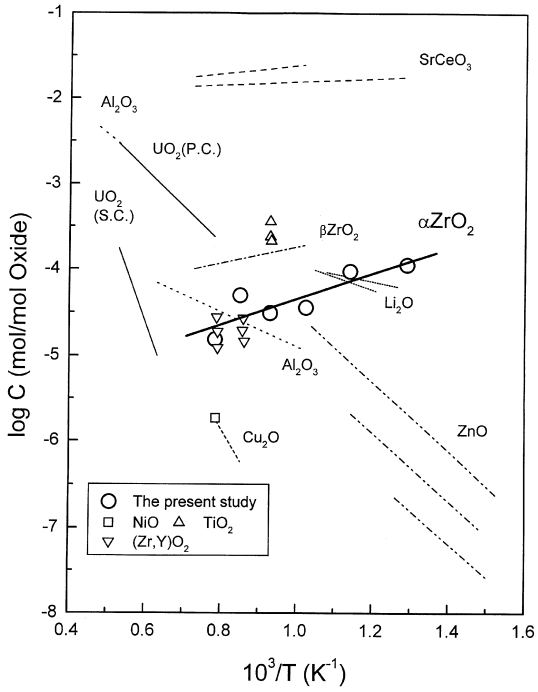

Fig. 14. Temperature dependence of the hydrogen solubility in ZrO_2.

The isothermal section of the Zr–O–H ternary system at 700°C was constructed from hydrogen pressure–hydrogen concentration isotherms for Zr(O) solid solutions. Oxygen was found to increase the terminal solubility in the α solution at the boundary between the α and α + β phases.

The hydrogen dissolution into the ZrO_2 oxide was examined in oxygen/water vapor atmosphere by means of the thermal desorption method. The thermal desorption of H_2O gas from the hydrogenated ZrO_2 was observed. The hydrogen solubilities in the ZrO_2 evaluated from the thermal desorption spectra were found to be from 10^{-5} to 10^{-4} mol H/mol oxide and to decrease with increasing temperature. The equilibria between the atmosphere and the complex oxide were able to be interpreted in terms of reactions involving oxygen vacancy and interstitial hydrogen defect.

Acknowledgements

It is a great honor for the authors to be given this opportunity to submit the present paper to the special issue of Professor Dr Olander. The authors gratefully acknowledge valuable and helpful discussions with Professor Dr Olander during the work on the Zr–O–H system. The present study has been performed under the

auspices of the Japan Atomic Energy Research Institute and partly supported by a Grant-in-Aid for Scientific Research from the Ministry of Education, Science and Culture.

References

[1] C.E. Ells, A.D. McQuillan, J. Inst. Met. 85 (1956) 89.
[2] K. Watanabe, J. Nucl. Mater. 136 (1985) 1.
[3] M. Someno, J. Jpn. Soc. Met. 24 (1955) 136.
[4] E.A. Gulbransen, K.F. Andrew, J. Met. 7 (1955) 136.
[5] M.W. Mallet, W.M. Albrecht, J. Elechrochem. Soc. 104 (1957) 142.
[6] R. Rica, T.A. Giorgi, J. Phys. Chem. 71 (1967) 3627.
[7] M. Tada, Y.C. Haung, Titanium–Zirconium 19 (1971) 260.
[8] M. Nagasaka, T. Yamashina, J. Less-Common Met. 45 (1976) 53.
[9] E. Zuzek, Surf. Coating Technol. 28 (1986) 323.
[10] E. Zuzek, Bull. Alloy Phase Diagrams 11 (1990) 385.
[11] W.-E. Wang, D.R. Olander, J. Am. Ceram. Soc. 78 (1995) 3323.
[12] M. Moalen, D.R. Olander, J. Nucl. Mater. 178 (1991) 161.
[13] K. Park, D.R. Olander, J. Am. Ceram. Soc. 74 (1991) 72.
[14] S. Yamanaka, T. Tanaka, M. Miyake, J. Nucl. Mater. 167 (1989) 231.
[15] S. Yamanaka, Y. Sato, H. Ogawa, M. Miyake, J. Nucl. Sci. Technol. 28 (1991) 135.
[16] S. Yamanaka, M. Miyake, J. Nucl. Mater 201 (1993) 134.
[17] S. Yamanaka, K. Higuchi, M. Miyake, J. Alloys Compounds 231 (1995) 503.
[18] S. Yamanaka, M. Miyake, M. Katsura, J. Nucl. Mater. 247 (1997) 315.
[19] S. Yamanaka, T. Nishizaki, M. Uno, M. Katsura, J. Alloys and Compounds (Proc. Int. Symp. Metal–Hydrogen Systems) to be published.
[20] T.B. Masalski, Binary Alloy Phase Diagrams, 2nd ed., ASM, Ohio, 1992.
[21] T.S. Elleman, D. Rao, K. Verghese, L. Zumawalt, DE-AS05-76-ET52022, DOE.
[22] C. Wagner, Ber. Bunsenges. Phys. Chem. 72 (1968) 778.
[23] S. Stotz, C. Wagner, Ber. Bunsenges. Phys. Chem. 70 (1966) 778.
[24] D.G. Thomas, J.J. Lander, J. Chem. Phys. 25 (1956) 1143.
[25] S. Yamanaka, M. Okada, S. Komatuki, M. Miyake, J. Alloys Compounds 231 (1995) 713.
[26] D.F. Sherman, D.R. Olander, J. Nucl. Mater. 166 (1989) 307.